

# Reynolds Number and Geometry Configuration Effect on Secondary Flows in S-Shaped Circular Bends

O. Ayala<sup>1\*</sup>, M.F. Degenring Oliveira<sup>2</sup>, P. Loures<sup>2</sup>

<sup>1</sup>Engineering Technology Department, Old Dominion University, Norfolk VA, USA

<sup>2</sup>Brazil Scientific Mobility Program, CAPES, Brasilia DF, Brazil

\*oayala@odu.edu

**Abstract:** Numerical simulations of a water flow in a circular three-dimensional S-shaped bend with sweep angles of 22.5, 45 and 90 degrees were executed at Reynolds numbers of 100, 1000, 10000, and 100000, with curvature ratio of 1.5D, 6.5D, and 10D. Simulations were made using COMSOL Multiphysics to analyze the influence of each of these parameters on the secondary flows and vorticity. In some cases, two pair of vortices was found, phenomena that if predictable, can be a solution to reduce erosion in all industry that use curved pipes.

**Keywords:** S-shaped bends, Secondary Flows, Vorticity.

## 1. Introduction

What do some industrial pipe layouts, heat exchangers, and arteries have in common? They all have S-shaped bend configurations. The formation of secondary flows is well known in such bends. In many situations, those flows have been used to enhance mixing and heat transfer. However, if particles are present in the fluid, those secondary flows could bring the particles closer to the pipe walls enhancing erosion. Billions of dollars have been spent every year due to the negative effects of corrosion and erosion in the oil & gas and power generation industries. The understanding of the secondary flow development inside S-shaped circular bends is helpful for future studies in S-shaped arteries and industrial pipeline erosion phenomena.

Most of the studies in S-shaped bends have focused on laminar flows, as they were interested in human bodies arteries (Hoogstraten et al., 1996; Johnston and Johnston, 2008; Niazmand and Jaghargh, 2010). Few have considered such configurations for a turbulent flow but they either have been for non-circular cross sections (Ng and Birk, 2013; Debnath et al. 2015), looked into the primary flow only (Mazhar et al., 2014), or were done for limited Reynolds number values (Taylor, 1984). In contrast to all previous studies, we propose to investigate how the

secondary flow develops along the S-shaped bends for: four different Reynolds numbers (100; 1,000; 10,000; and 100,000), three radius of curvature ( $r/D= 1.5, 6.5,$  and  $10$ ), and three sweep angles (22.5, 45, and 90 degrees).

Simulations were performed with COMSOL Multiphysics 5.1 using the CFD module to analyze the secondary flows and vorticity magnitude profile on cut planes along the bends. A model validation was created using a three-dimensional S-shaped bend with sweep angle of 90°, radius of curvature ( $r/D$ ) of 6.5, and Reynolds number of 960 as presented by Niazmand and Jaghargh (2010).

## 2. Physical Model

The most common geometrical parameters used to characterize a steady flow in a curved pipe are Reynolds number, sweep angle and curvature radius. With this in mind, nine different geometries of consecutive bends were considered, with three distinct sweep angles (22.5, 45 and 90 degrees), and three curvature ratio (1.5D, 6.5D, and 10D), where D is the pipe diameter, which is 0.00127 m. An inlet pipe of 6D was simulated to ensure fully developed flow in the beginning of the first bend and a straight outlet pipe was designed to visualize the parameters effects after the second elbow exit.

For each bend configuration, the steady flow for water was studied for four Reynolds numbers, two laminar cases, 100 and 1 000, and two turbulent cases, 10 000 and 100 000. The distance of six times the diameter (6D) was used for the pipe connected to the bend inlet, which was found to be enough to eliminate any entrance length effect.

## 3. Mathematical and Numerical Model

The simulation was designed to consider the fluid as homogenous, single-phase, incompressible and Newtonian with properties of water under steady-state conditions. The three-dimensional Navier-Stokes equations were

solved using COMSOL Multiphysics through its Fluid Flow Module.

For the inlet condition, a velocity profile was defined to help even more to eliminate any entrance length effect in the bend. The laminar flow cases followed the corresponding parabolic profile and for the turbulent cases a profile were obtained taking the exit velocity profile in a long pipe fluid flow simulation. As for the outlet, the pressure was set to zero and an outlet location sensitivity analysis was developed to ensure it would not affect the bend flow behavior.

The model used to compare against previous results by Niazmand and Jaghargh (2010) for a steady-flow in S-shaped bends. The chosen geometry consisted of double bends with sweep angles of 90 degrees and Reynolds number of 960. The results obtained for non-dimensional axial velocity in different cross sections along the geometry were really similar to the one published by those authors.

Mesh sensitivity analysis (for both element size and wall resolution) was carefully performed. The normal mesh provided by COMSOL was found to be the most suitable since its results had less than 5% of difference when compared with finer and run much faster. For the turbulent cases, the k-ε model was used. The boundary elements were adjusted in order to decrease wall lift-off values to 11.6 (viscous unit).

#### 4. Results and Discussion

In order to better compare the effect of the geometry and the Reynolds Number on the fluid behavior, normalization was chose to transform the results into nondimensional values. The velocity and vorticity are normalized with  $U_{mean}$  and  $U_{mean}^*/D$ , respectively. For laminar cases,  $U_{mean}^*$  is defined as the average inlet velocity. For the turbulent cases,  $U_{mean}^*$  is half of the maximum velocity magnitude in the system. The values of  $U_{mean}^*$  for each case are shown in the table 1.

The simulation in a S-shaped configuration with Reynolds number equal to 10,000; sweep angles of 90 degrees and 1.5D ratio of curvature was considered as the base model of our study. An investigation varying the sweep angles, radius of curvature and Reynolds Numbers was done to analyze the influence on the secondary flows and vorticities.

Table 1: Normalization factors

Re	SA	CR	$U_{mean}^*$ (m/s)
100	All Cases		0.0040
1,000	All Cases		0.0395
10,000	22.5	1.5	0.240
		6.5	0.230
		10	0.225
	45	1.5	0.270
		6.5	0.226
		10	0.220
	90	1.5	0.305
		6.5	0.224
		10	0.218
100,000	22.5	1.5	2.283
		6.5	2.195
		10	2.160
	45	1.5	2.614
		6.5	2.190
		10	2.125
	90	1.5	2.883
		6.5	2.183
		10	2.118

The results were analyzed using table pictures, where the flow goes away from the reader, as shown in Figure 1. The bottom half of the plot represents the inner section of the first bend and the outer section of the second bend, while the upper half of the plot shows the outer section of the first bend and the inner section of the second bend.

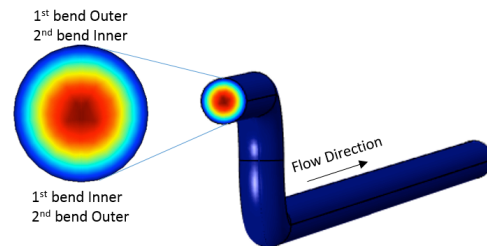
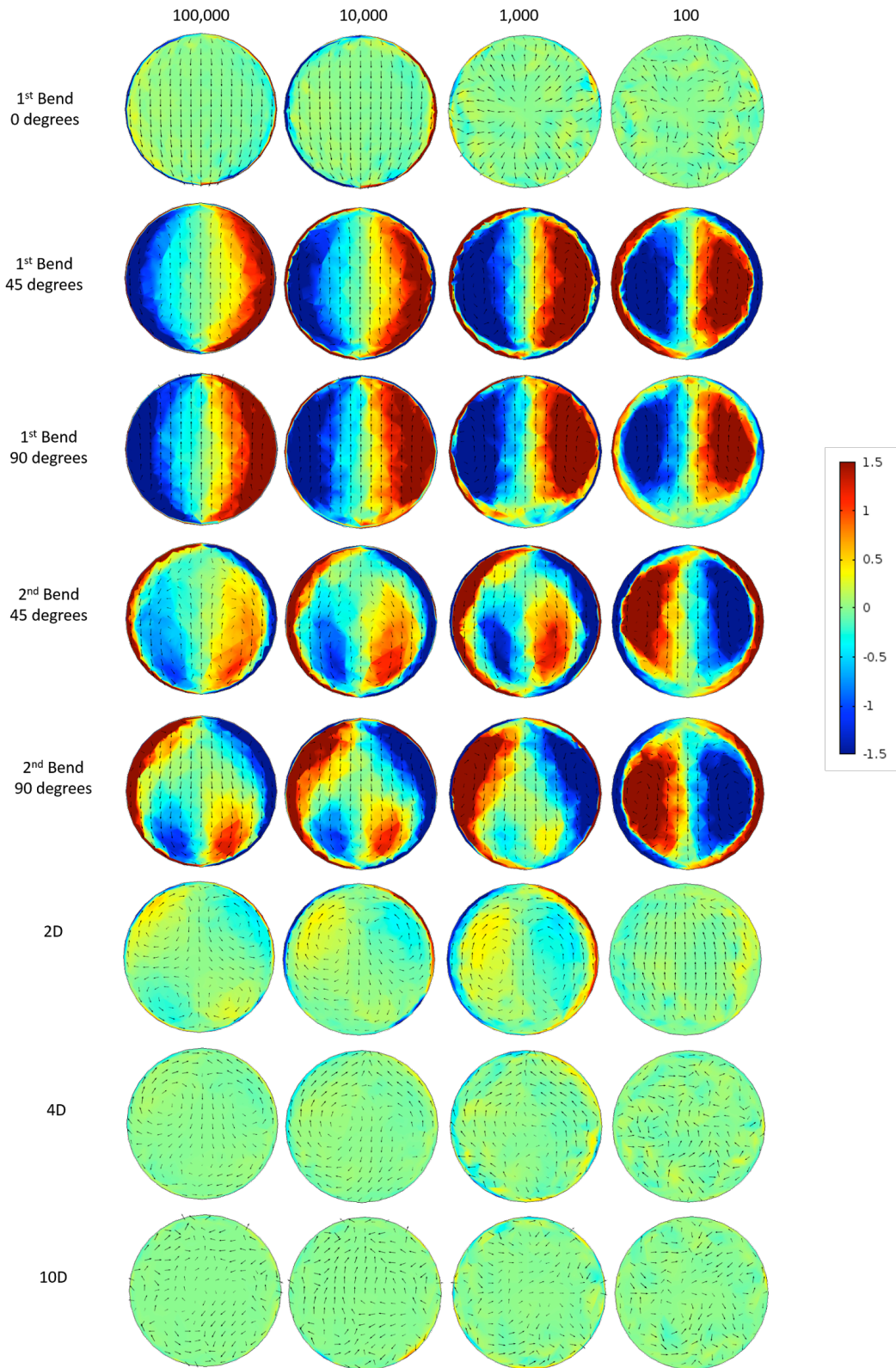


Figure 1. View of each cut plane.

It is important to mention that the vector length in the figures do not intend to demonstrate directly the magnitude of the velocities, just its direction and behavior. In addition, the vorticity magnitude is shown by colors. Red indicates that the vorticity vector is in the same direction of axial fluid flow, while blue colors indicates otherwise.

##### 4.1. Reynolds Number Effect

In figure 2 shows the effect of Reynolds number on the secondary flows for some selected bend cross sections. We show in-plane



**Figure 2:** Effect of Reynolds Number on the vorticity and secondary flows for geometries with 1.5D ratio of curvature and 90 degrees sweep angle.

velocities represented by the vectors and also show the in-plane vorticity magnitude represented by the colors.

At the inlet of the first bend, there is no clear secondary flow and it is a weak flow. However, a pair of vorticity fields starts to grow close to the wall for all Reynolds number cases. Since at the inlet there are no centrifugal forces yet, the appearance of the vorticity fields could be related to the already formed secondary flows downstream inside the bend. Downstream fluid flow could affect upstream fluid flow due to fluid continuity.

As the flow moves down into the bend, centrifugal forces start to act on the fluid and secondary flows are formed. The rotating flow makes the fluid particles to rotate as well developing the vorticity fields. Note in the figure that the vorticity field direction and the secondary flow rotational direction are aligned, thus they are correlated. There is another pair of vorticity fields very near the wall rotating in an opposite direction, which gets formed due to the rapid change of the secondary flow velocity to zero at the wall.

Examining figure 2, it can be noted that the main impact of Reynolds number is the how close the secondary flow structure and/or vorticity field is to the wall. As Reynolds Number is increased, the pair of vorticities stays longer attached to the wall, most likely due to the increasing fluid inertial forces.

When the fluid enters the second bend, the centrifugal forces change direction creating secondary flows in an opposite direction developing from the wall and at the inner section of the second bend. The first pair of secondary flows (or vorticity fields) gets detached from the wall, gradually losing its strength while the newly formed second pair intensifies and wraps the first pair. The first pair gets pushed to the outer section of the second bend by the fluid at the core moving in the centrifugal force direction. In addition, since the centrifugal forces are stronger for higher Reynolds numbers, the strong secondary flows from the first bend dominate forcing a delay on the formation of the new pair of secondary flows.

For low Reynolds number ( $Re = 100$ ), the second pair of vorticity seems to completely annihilate the first pair inside the second bend. This was observed by Hoogstraten *et al.* (1996) who found that for  $Re < 240$  no traces of the

secondary vortices created in the first bend are visible at the end of the second bend. Additional vorticity profiles at different angles between the end of the first bend and the middle of the second bend were examined (not shown) and it was observed that similar phenomena of first pair of vorticity detaching from wall and going to the center, and second vorticity pair generation and grow, very similarly what was observed for higher Reynolds Number. Therefore, the phenomena still occurs but much quickly and with weaker intensity.

A final observation is that when the fluid leaves the second bend, there are no centrifugal forces acting anymore but the fluid still rotates (see vectors) because of the fluid inertia.

## 4.2. Geometry Effect

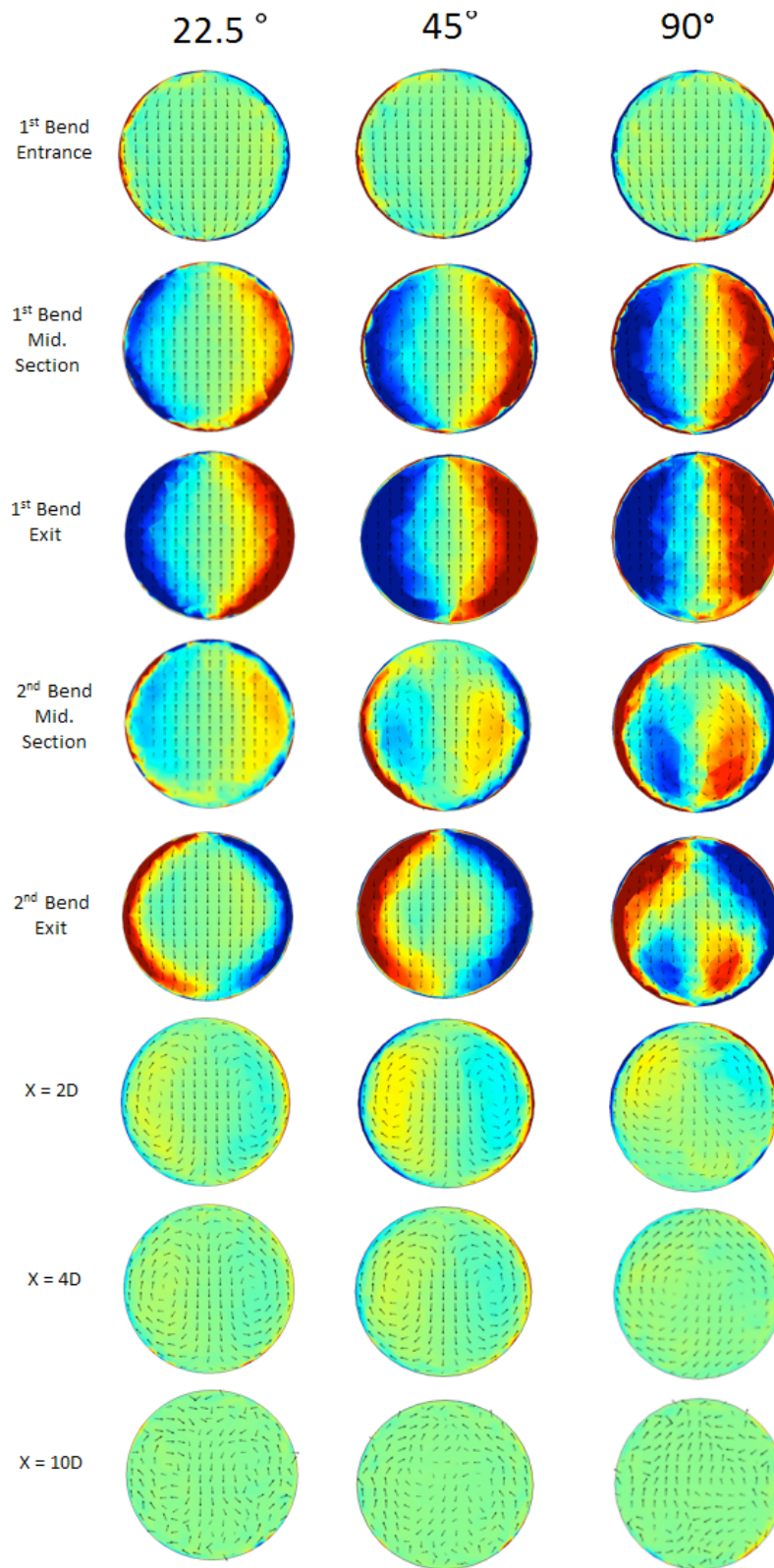
### 4.2.1. Sweep Angle Effects

Figure 3 shows the vorticity field and secondary flows for different bend sweep angles and a fixed Reynolds number equal to 10,000 and 1.5 curvature radius. The larger the sweep angle, the stronger the vorticity magnitude and secondary flows. The main effect of the sweep angle is related to the fluid residence time, as it is larger with sweep angle. The higher the time the fluid stays inside the bend, the larger centrifugal force effect.

### 4.2.2. Curvature Radius Effect

Analyzing the numerical results it was found that the maximum axial velocity magnitude is inversely proportional to the curvature radius. For the simulation with 1.5D, the maximum velocity was 1.6 times the average inlet velocity, but for the cases with 10D, the maximum velocity was 1.1 times the average velocity. The point of maximum axial velocity magnitude is in the inner part of the second bend for all cases.

For 1.5D curvature radius, there appears a detachment from the wall near to the outer part of the second bend. For the case of Reynolds Number of 1,000, and 45 and 90 degrees, there even occurs a backflow of very low magnitude, 2.6% and 2.1%, respectively. Figure 4 shows the axial velocity magnitude for 1.5D, 90 degrees and 1,000 Reynolds Number. For higher  $r/D$ , the detachment from the wall in the outer part of the second bend is subtle with no backflow.



**Figure 3:** Effect of sweep angle on the vorticity for geometries with 10,000 Reynolds Number and 1.5D curvature radius.

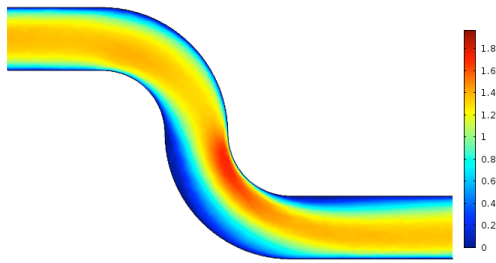


**Figure 4.** Axial velocity magnitude for curvature radius of 1.5D, 90 degrees sweep angle and 1,000 Reynolds Number.

Figure 5 shows the vorticity magnitude field and secondary flows for different curvature radius and fixed Reynolds number equal to 10,000 and sweep angle of 90 degrees. It can be noticed that the smaller curvature radius, the stronger the vorticity field (and secondary flows), and the longer the second pair of secondary flows takes to develop. The centrifugal forces are responsible of strengthen the secondary flows and its magnitude increases with the inverse of curvature radius.

A final observation for 1.5D curvature radius is that after the fluid leaves the second bend, a new pair of secondary flows appears even though no centrifugal forces are acting anymore. This is due to the remaining vorticity field (generated in the first bend) at the second bend exit.

## 5. Conclusion

Based on the observations explained above, it can be seen that the pipe geometry and fluid Reynolds number influences the particle fluid behavior, its vorticity and secondary flows.

**Reynolds Numbers:** In the first bend, the higher the Reynolds number, the longer the first pair of vorticities stays attached to the wall. In the second bend, the higher Reynolds Numbers, the secondary flow from the first bend dominates, longer it will take for the second pair of secondary flows to develop.

**Curvature Radius:** The smaller the curvature radius is, the stronger the vorticity magnitude is, and longer it will take for the second pair of secondary flows to develop.

**Sweep Angles:** The larger the sweep angle, the stronger the vorticity magnitude is and longer it lasts.

For all Reynolds Numbers we have studied, at some point, the first pair of vorticity fields start to detach from the wall and a second pair of vorticity appears wrapping the first one, which decreases intensity (sometimes completely annihilated) and goes to the center and in the direction of the secondary flow.

In some turbulent cases there was the formation of 4 vortices at the outlet pipe. The first pair of vorticities were generated because of inertia and the second pair had appeared because translation and rotation in opposite directions of the first pair of vorticity field. Additional study is necessary to track these vortices and apply the results to the industry.

## 6. References

1. Hoogstraten, H. W., J. G. Kootstra, B. Hillen, J. K. B. Krijger, and P. J. W. Wensing. Numerical simulation of blood flow in an artery with two successive bends, *J. Biomech.* **29**, 1075–1083, (1996)
2. Johnston, P. R., and B. M. Johnston. Blood flow in S-shaped in-plane and out-of-plane coronary arteries. *ANZIAM*, **49**, 341–358, (2008)
3. Niazmand H., Jaghargh E.R.. Bend sweep angle and Reynolds number effects on hemodynamics of s-shaped arteries. *Ann Biomed Eng*, **38(9)**, 2817–2828, (2010)
4. Ng, Billy C. N. and Birk, A. M.. Experimental and CFD study of a rectangular s-bend passage with and without pressure recovery effects. *Proceedings of the Asme Turbo Expo: Turbine Technical Conference and Exposition*, San Antonio, TX, Amer Soc Mechanical Engineers, (2013)
5. Mazhar, H. , Ewing, D. , Cotton, J. S. , and Ching, C. Y.. Mass transfer in dual pipe bends arranged in an S-configuration, *Int. J. Heat Mass Transfer*, **71**, pp. 747–757, (2014)
6. Debnath, R., Mandal A., Majumder S., Bhattacharjee S. and Roy D.. Numerical analysis of turbulent fluid flow and heat transfer in a rectangular elbow. *Journal of Applied Fluid Mechanics*, **8(2)**, 231–241, (2015)

## 7. Acknowledgements

The authors would like to thank the Brazil Scientific Mobility Program for sponsoring the Academic Training at Old Dominion University.

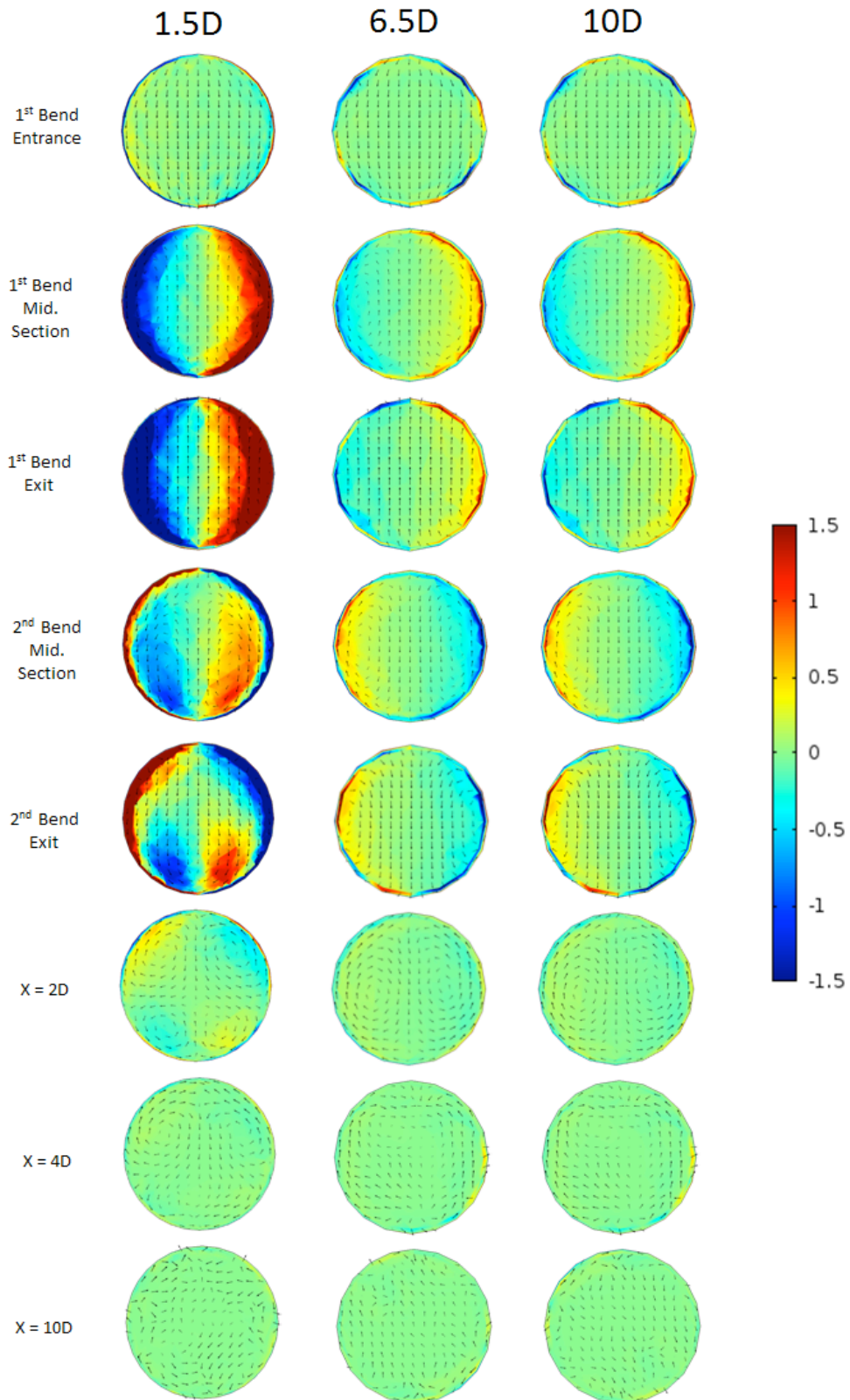


**Figure 5:** Effect of Curvature Radius on the vorticity for geometries with 10,000 Reynolds Number and 90 degrees sweep angle.